Permeability Variations During Crack Damage Evolution in Rocks

Philip Meredith

Mineral, Ice & Rock Physics Laboratory
Department of Earth Sciences
University College London

Euroconference, Erice, September 2007

Acknowledgements

Patrick Baud (EOST, Strasbourg)
Phil Benson (UCL & University of Toronto)
Steve Boon (UCL)
Oswald Clint (UCL)
Lun Li (Edinburgh University)
Ian Main (Edinburgh University)
Alexandre Schubnel (ENS, Paris)
Ben Thompson (University of Toronto)
Ed Townend (UCL)
Paul Young (University of Toronto)

OUTLINE

- Motivation for studying permeability evolution
- Permeability evolution near the crack percolation threshold
- Influence of void space geometry on permeability evolution under elevated isostatic pressure
- Permeability evolution during sequential propagation of compaction bands under deviatoric stress

MOTIVATION

- It is well known that no simple or general relationship exists between rock porosity and rock permeability.
- This is because porosity is simply a scalar measure of the relative volume of void space in a rock.
- By contrast, permeability is controlled by the way the individual void spaces are organised:
  i.e. their geometry and connectivity.
- In particular, we are interested in how permeability evolves and changes in response to changes in void geometry and connectivity caused by changes in pressure and deviatoric stress.

#1 Permeability evolution near the percolation threshold

Introduction

- Permeability
  - Controlled through interlinking of cracks and pores
  - Critical connection of cracks occurs at percolation threshold
  - Permeability sensitivity to crack density is maximum here
- Problem
  - We need to identify a 'damage free' rock
    - Isotropic and Homogeneous
    - Vanishingly small porosity and permeability
- Approach
  - Introduce 'damage' in controlled manner
  - Measure velocity and permeability changes at each stage
- Why?
  - Obtain a more detailed understanding of permeability evolution near the percolation threshold

Ailsa Craig Microgranite: the “nearly” perfect rock

The island of Ailsa Craig in the Firth of Clyde:

(approx. 250m high x 600m across)

A curling stone made from Ailsa Craig Microgranite (ACG): approx. 30cm in diameter.

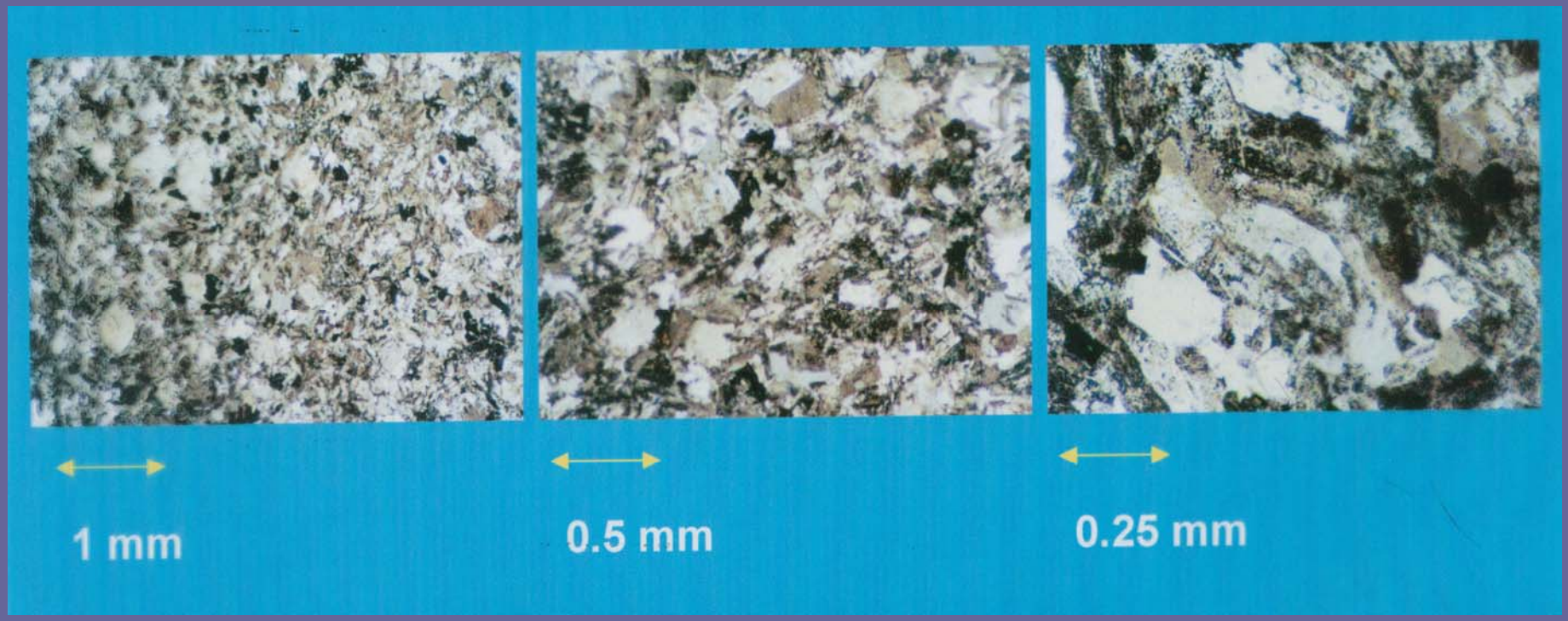

Thin section images of ACG at different scales showing that there are no discernible microcracks.

Ailsa Craig Microgranite (ACG)

Mineralogy	Volume %
Alkali Feldspar	73.3
Quartz	19.0
Amphibole	7.30
Apatite	0.40

Mean Grain Size	0.25mm

Physical Properties	(Untreated)
Porosity	< 1.00 %
Permeability	1.50×10^{-23} m^2
Mean P - wave velocity	5.30 km/s
Mean S - wave velocity	3.63 km/s
P-wave anisotropy	0.05%
S-wave anisotropy	0.08%

- Note the extremely low permeability in the "as-received" state
- Samples then slowly heated (1^0C/min) to induce thermal crack damage

Changes in wave velocities as a result of thermal stressing.

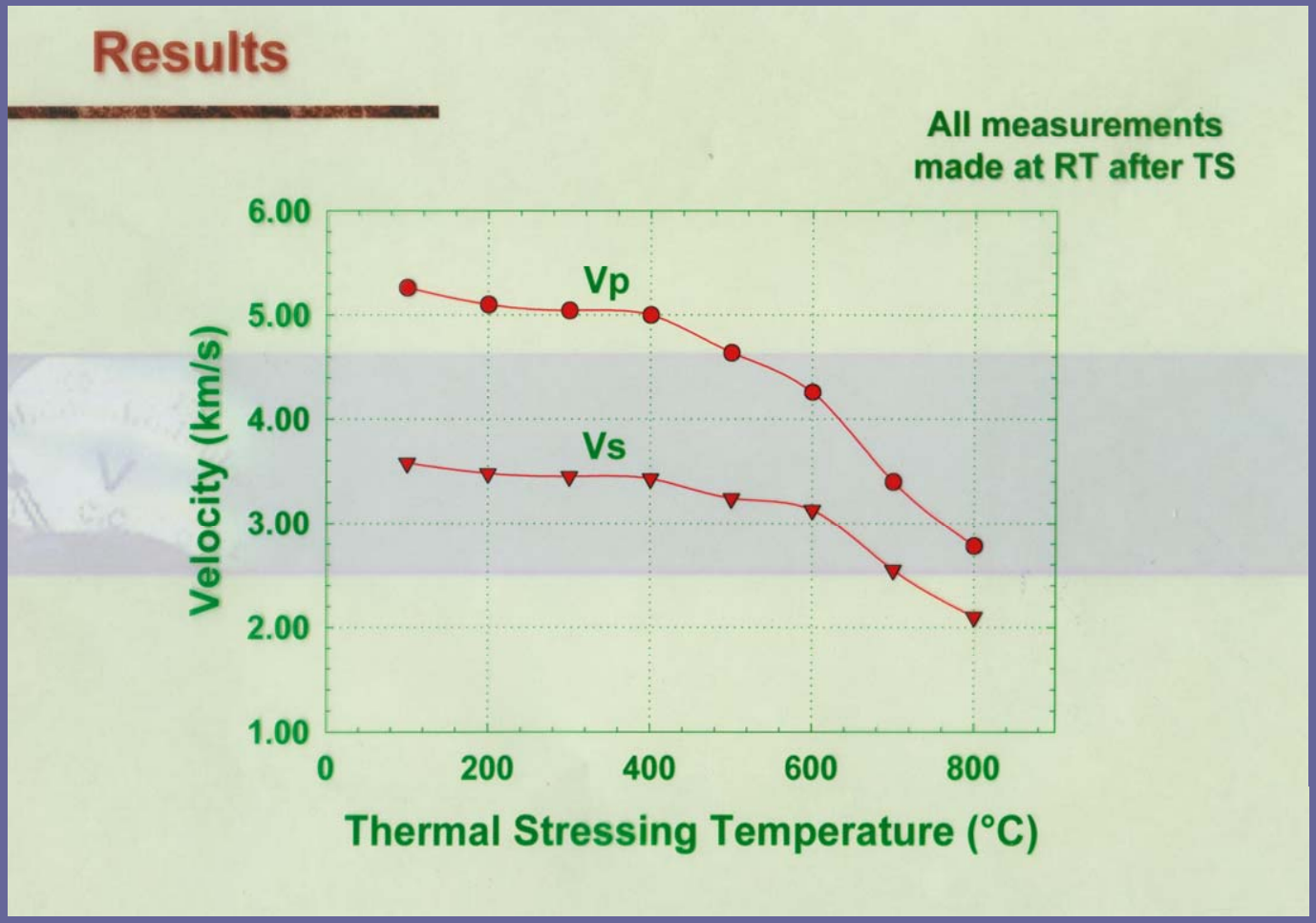

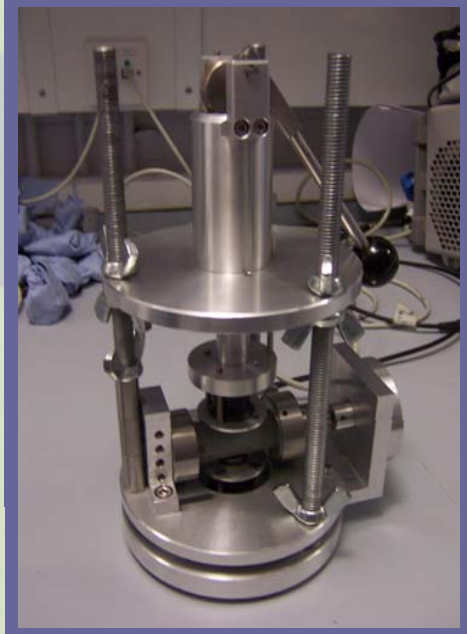

P and S Wave Velocity Anisotropy before and after Thermal Stressing

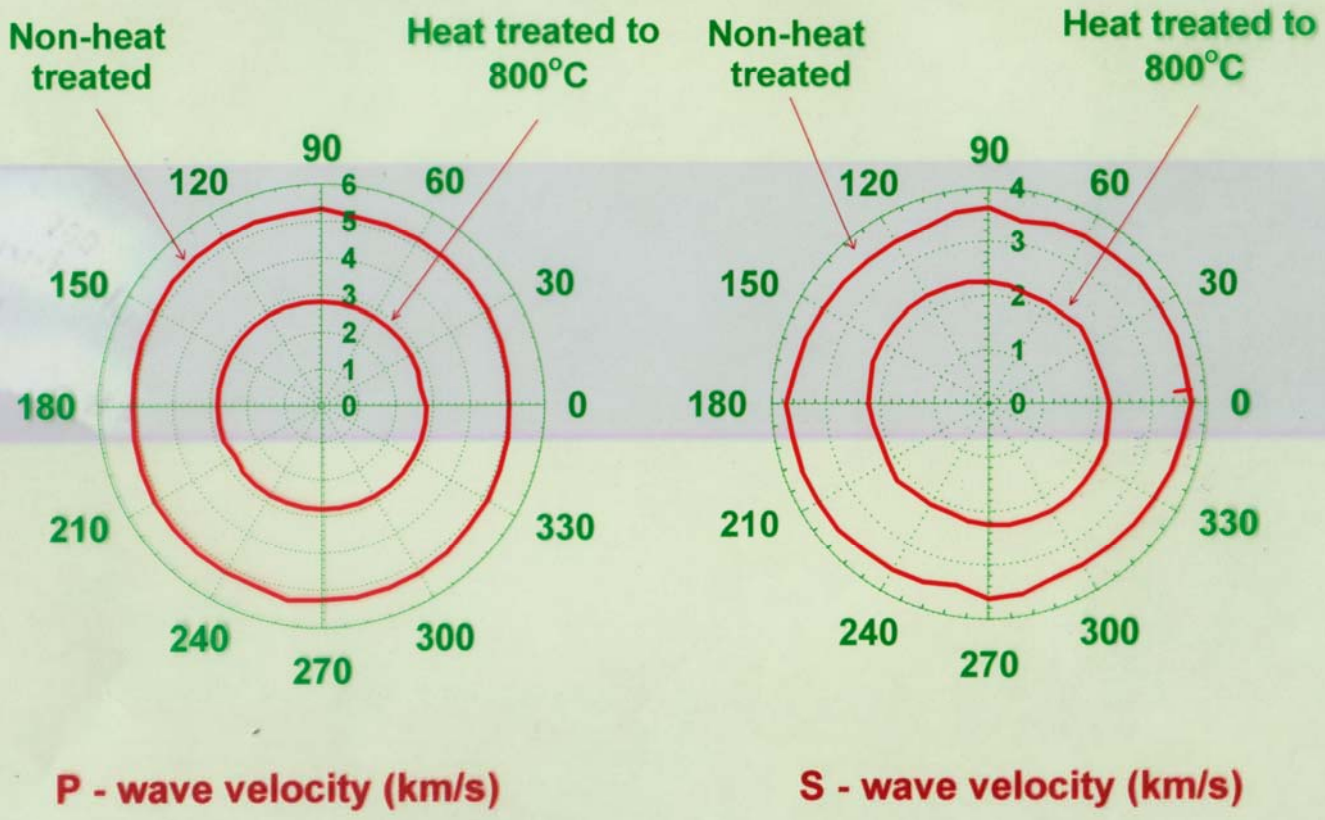

Large output of AE during TS suggests occurrence of thermal cracking

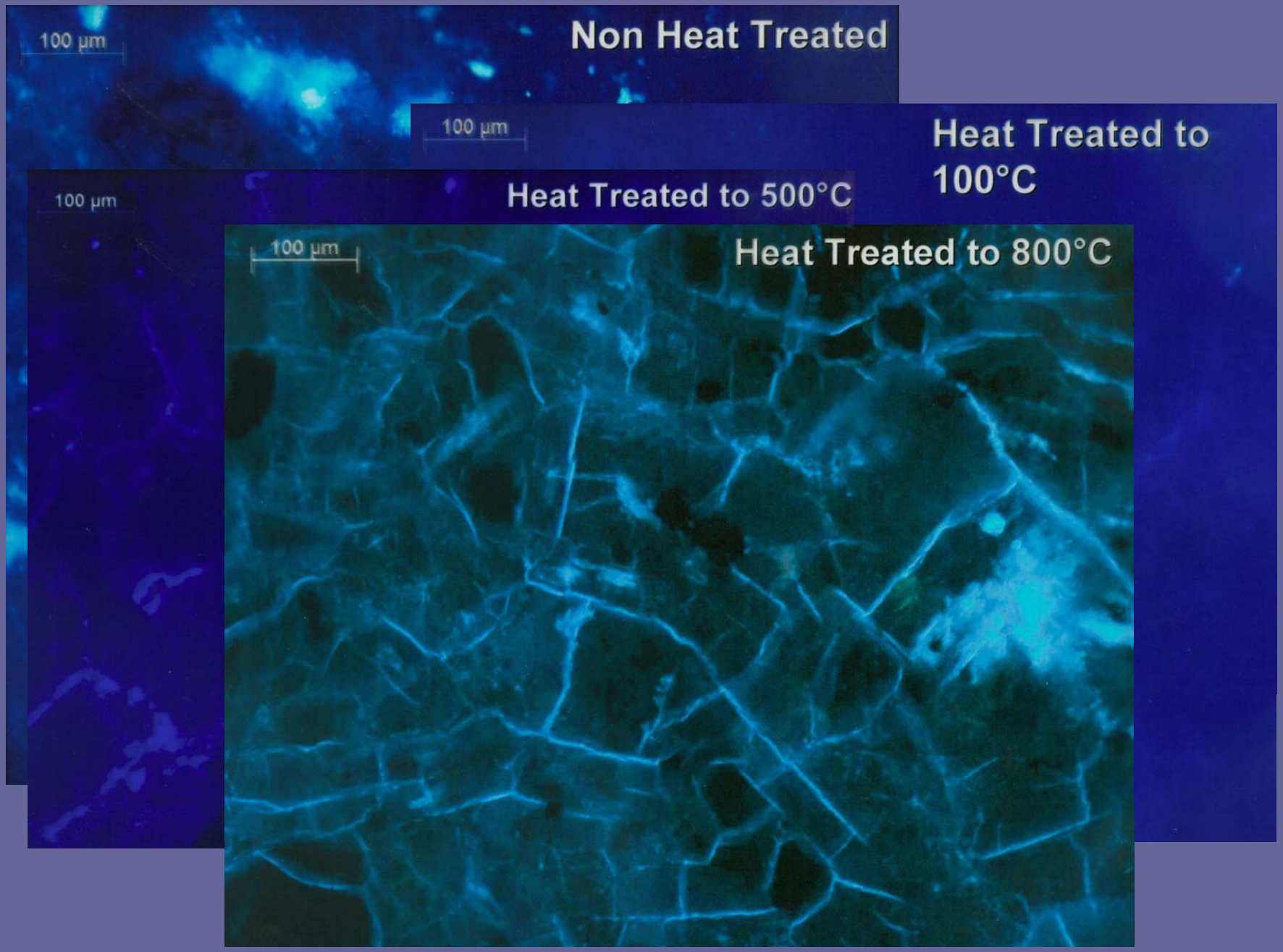
100 µm
Non Heat Treated
100 µm
Heat Treated to 100°C
100 µm
Heat Treated to 500°C
100 µm
Heat Treated to 800°C

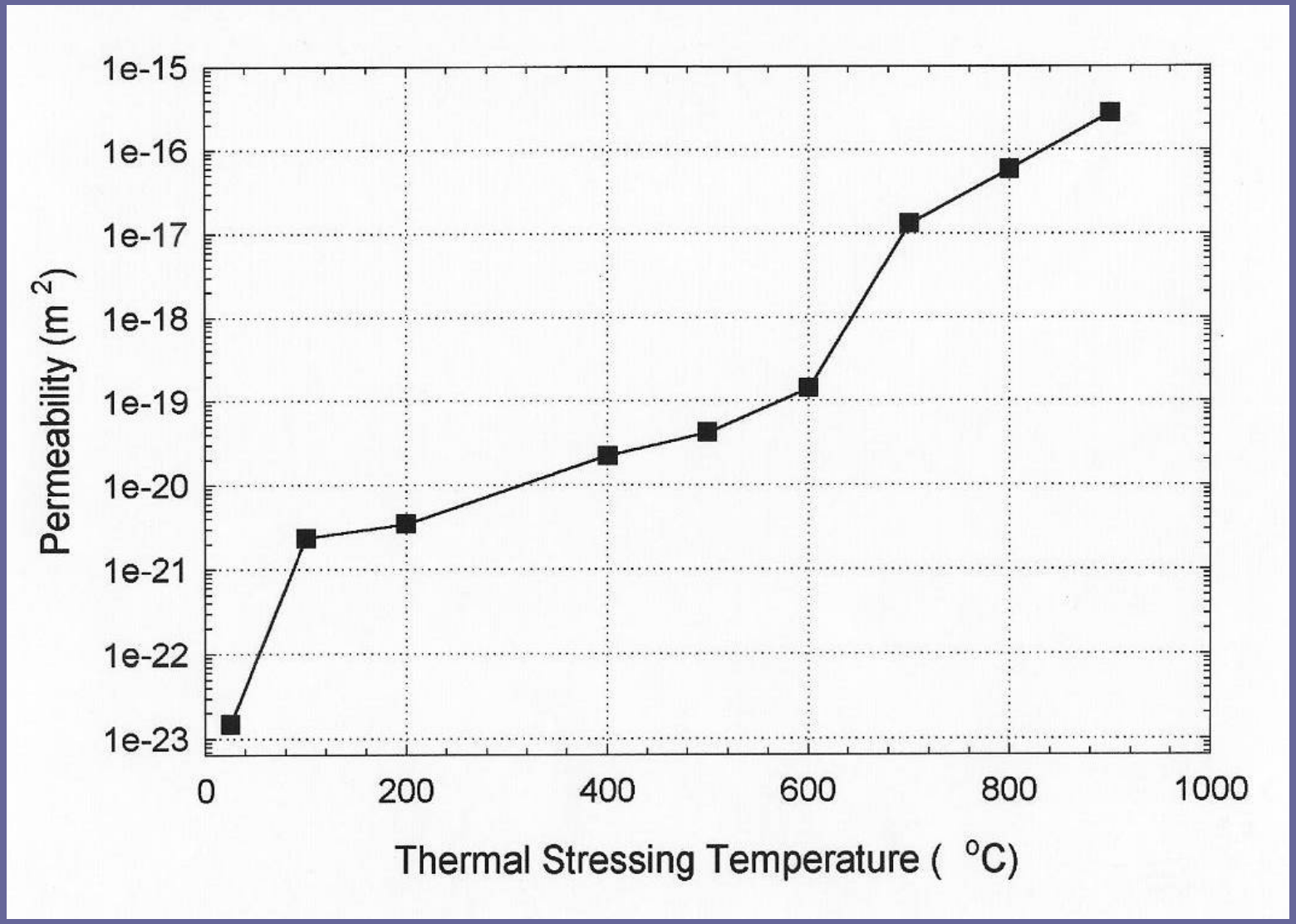

Thermal cracking increases permeability by > 7 orders of magnitude

Percolation Model

- Aim was to test the hypothesis that the porosity (Φ) – permeability (K) relation has the universal form expected for a system near the percolation threshold:

$$K = K_0 \left(\phi - \phi_C \right)^n \qquad \text{(equation 1)}$$

- This relation has been proposed previously on theoretical grounds, from network modelling and from empirical observations.

Porosity vs. Log Permeability for Thermally-Stressed ACG

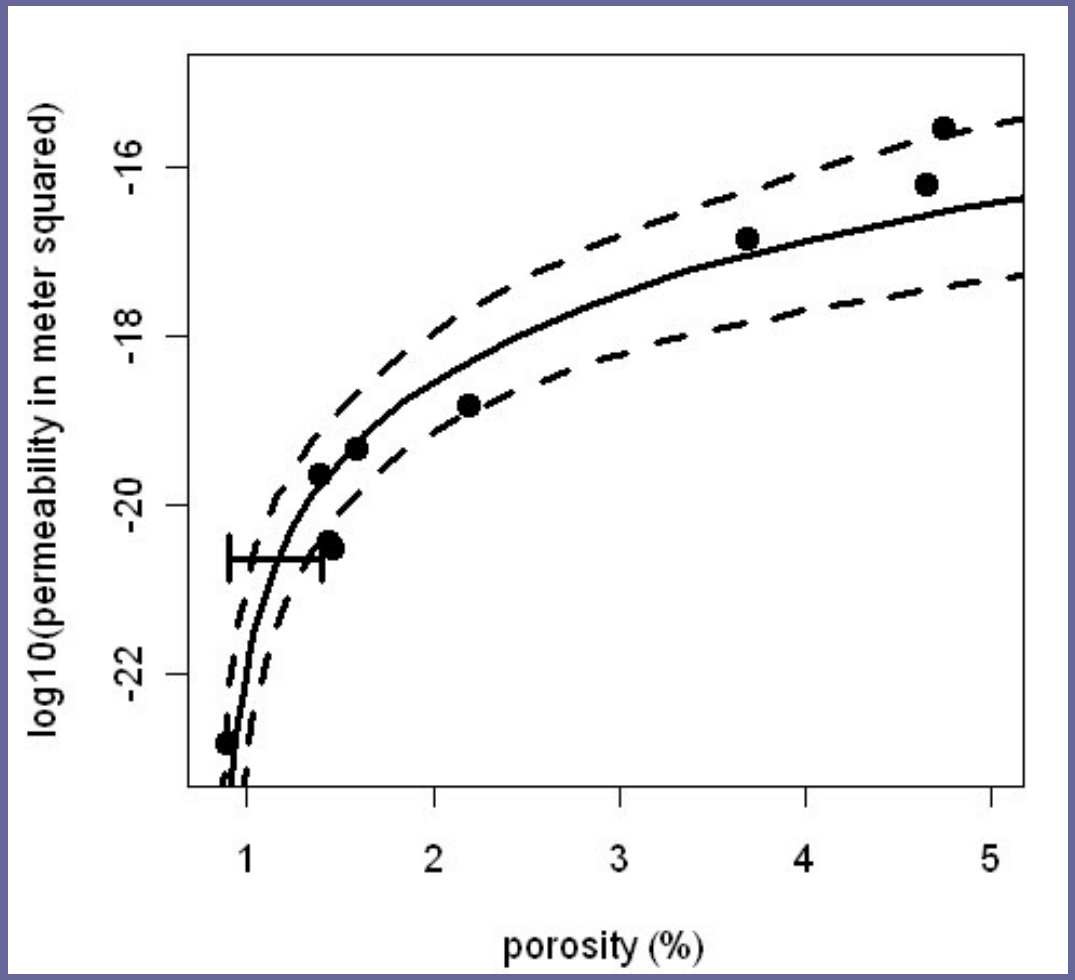

- Data define a single population
- Optimal value of threshold porosity (Φ_C) was 0.85
- Best fit curve is shown with 95% confidence limits
- Least squares fit gives best value of "n" as 3.79 ± 0.45
- $R^2 = 0.912$

(Meredith, Main, Clint & Li, 2007)

Summary #1

- The results confirm the hypothesis of equation 1.
- The high value of “n” is most consistent with the “Swiss Cheese” continuum percolation model of Feng et al. (*Phys. Rev. B, 35, 1987)*.
- A modest change on porosity from 1 to 5% therefore results in a massive change in permeability of > 7 orders of magnitude.
- This change and the high value of “n” are explained by the geometry of the microcrack network.

#2 Influence of void space geometry on permeability evolution under elevated isostatic pressure

APPROACH:

- Measure permeability as a function of effective pressure using the steady-state flow technique.
- Contemporaneously measure changes in Vp and Vs with increasing effective pressure.
- Use the *Kachanov* effective medium model to calculate crack densities and aspect ratios from the velocity data.
- Use the statistical model of *Gueguen & Dienes* to calculate permeability from the calculated crack parameters.
- Finally, compare the modelled permeabilities with the directly measured permeabilities.
- Apply the methodology to rocks with very different void space geometries.

Test material characteristics:

Crab Orchard sst. (COS) **Takidani granite (TDG)**

Φ = 4% **Φ = 1%**

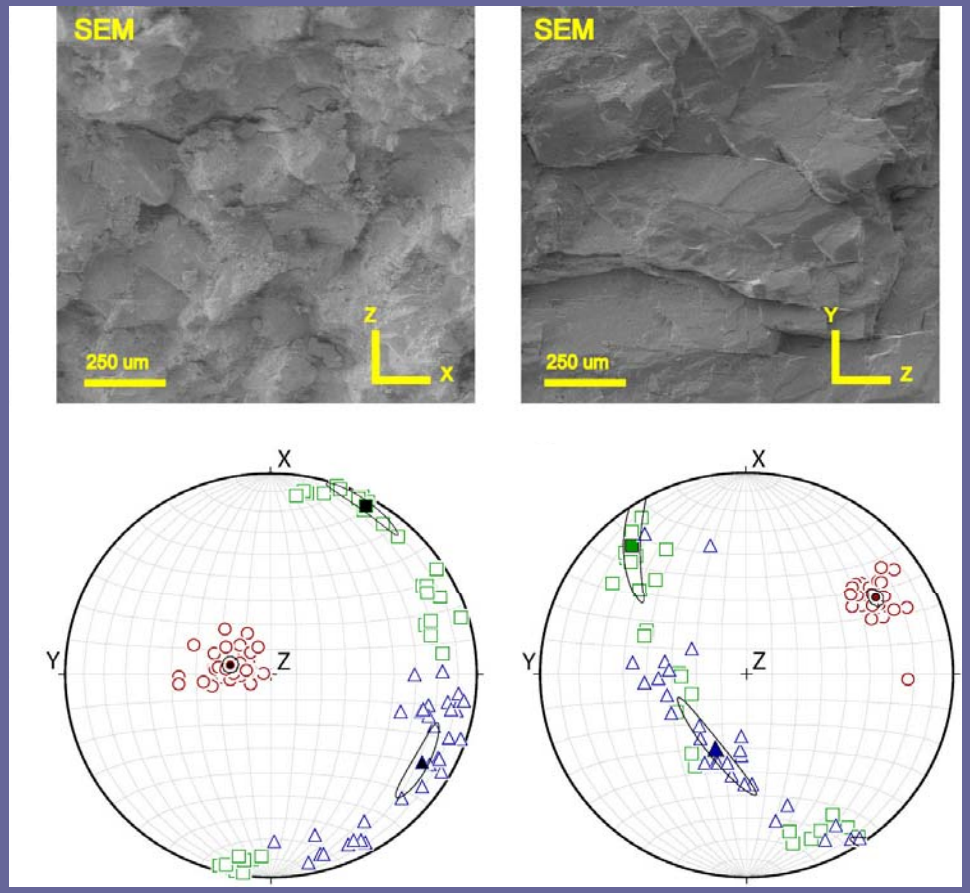

Pores + cracks **Aligned cracks**

Both materials exhibit transverse isotropy as indicated in the stereograms

Measurements of changes in wave velocities and permeability under isostatic pressure

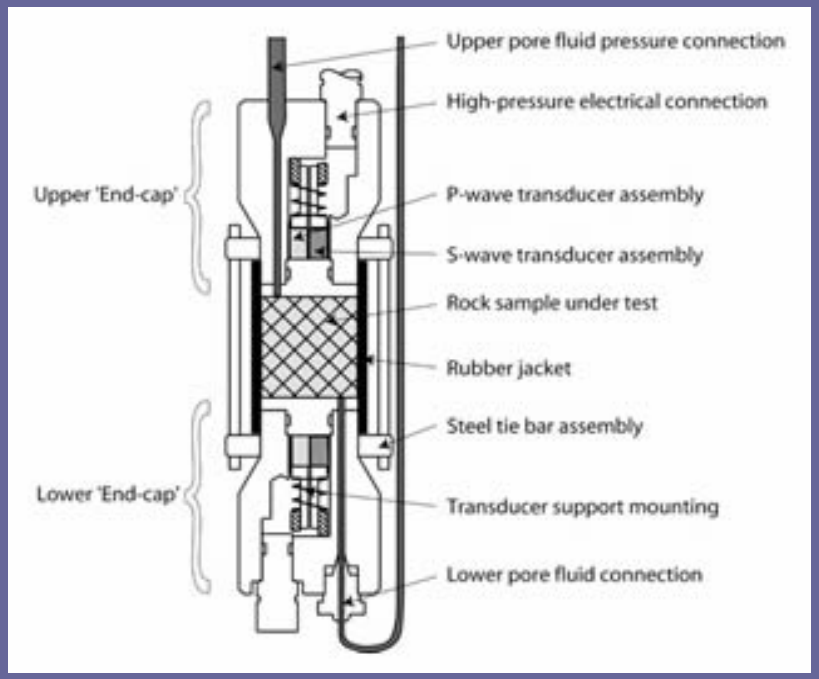

Permeameter with Vp and Vs measurement capability at UCL

Crab Orchard Sandstone

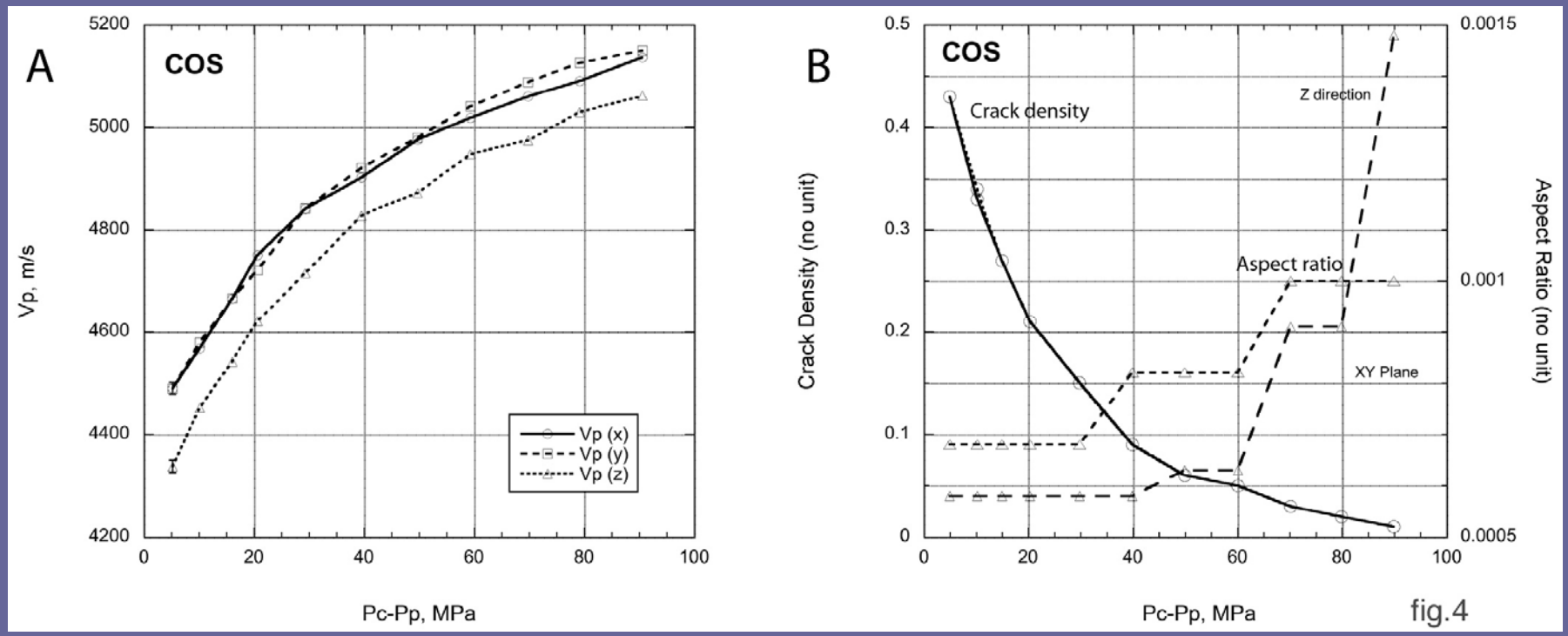

Benson, Meredith & Schubnel, JGR, 2006.

Measured increase in P-wave velocity with increase in effective pressure.

Calculated change in crack density and aspect ratio with increase in effective pressure.

Takidani Granite

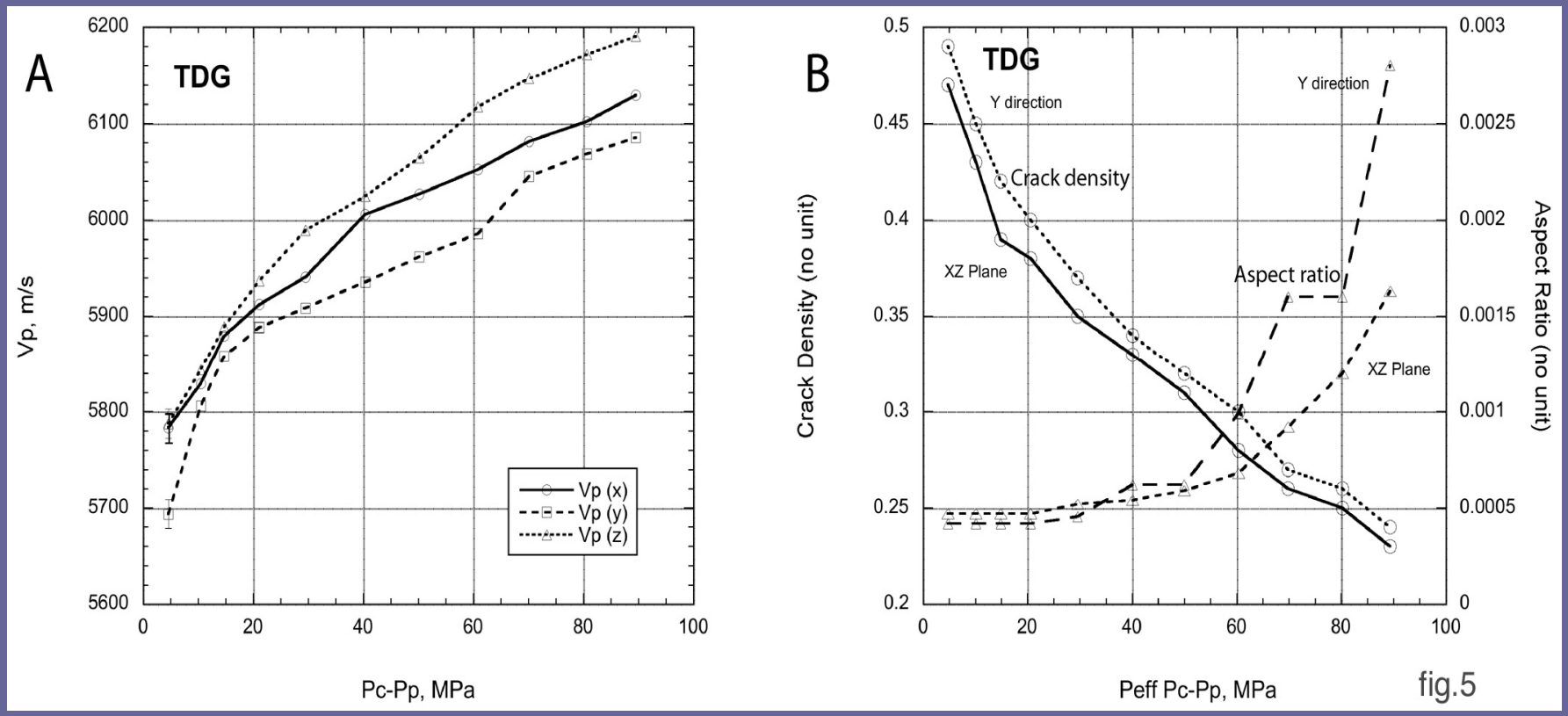

Measured increase in P-wave velocity with increase in effective pressure.

Calculated change in crack density and aspect ratio with increase in effective pressure.

Crab Orchard Sandstone

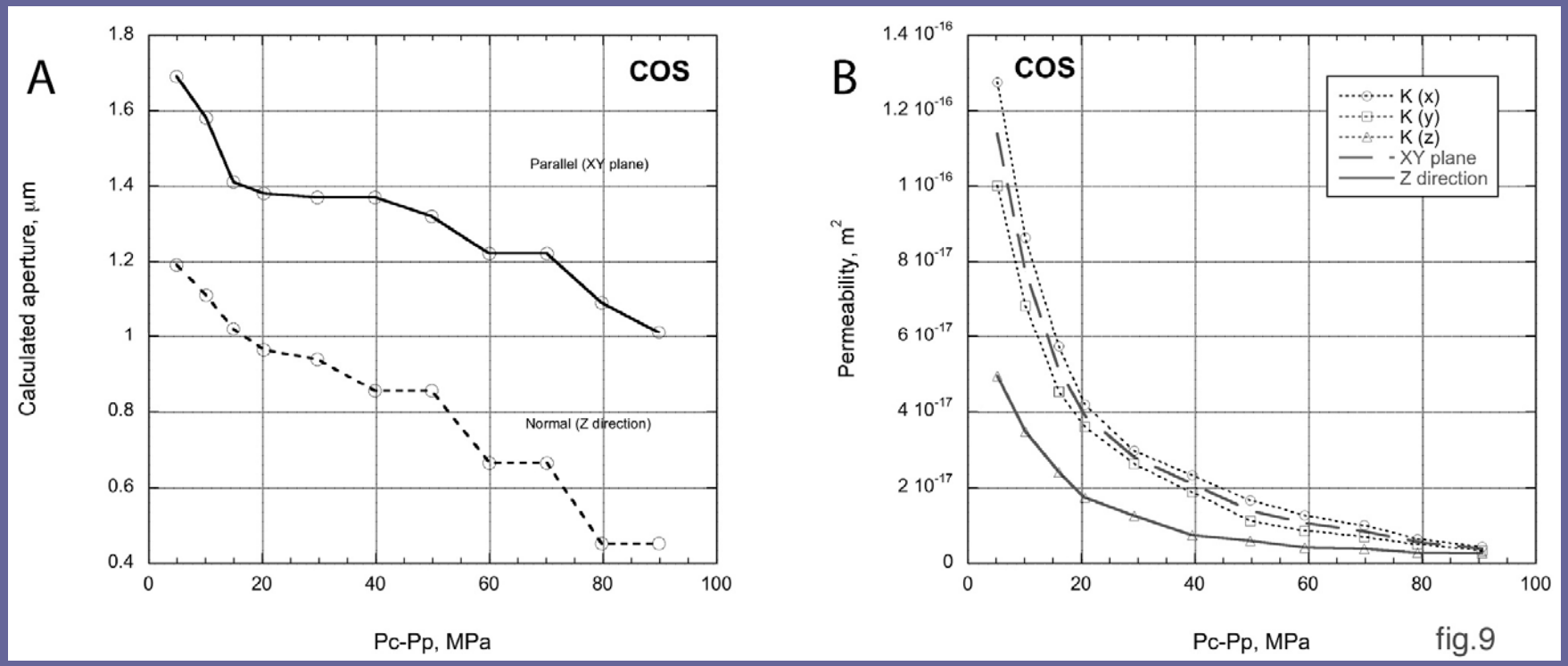

Calculated decrease in crack aperture with increase in effective pressure.

Comparison of measured (dotted lines) and modelled (dashed and solid lines) permeability.

Takidani Granite

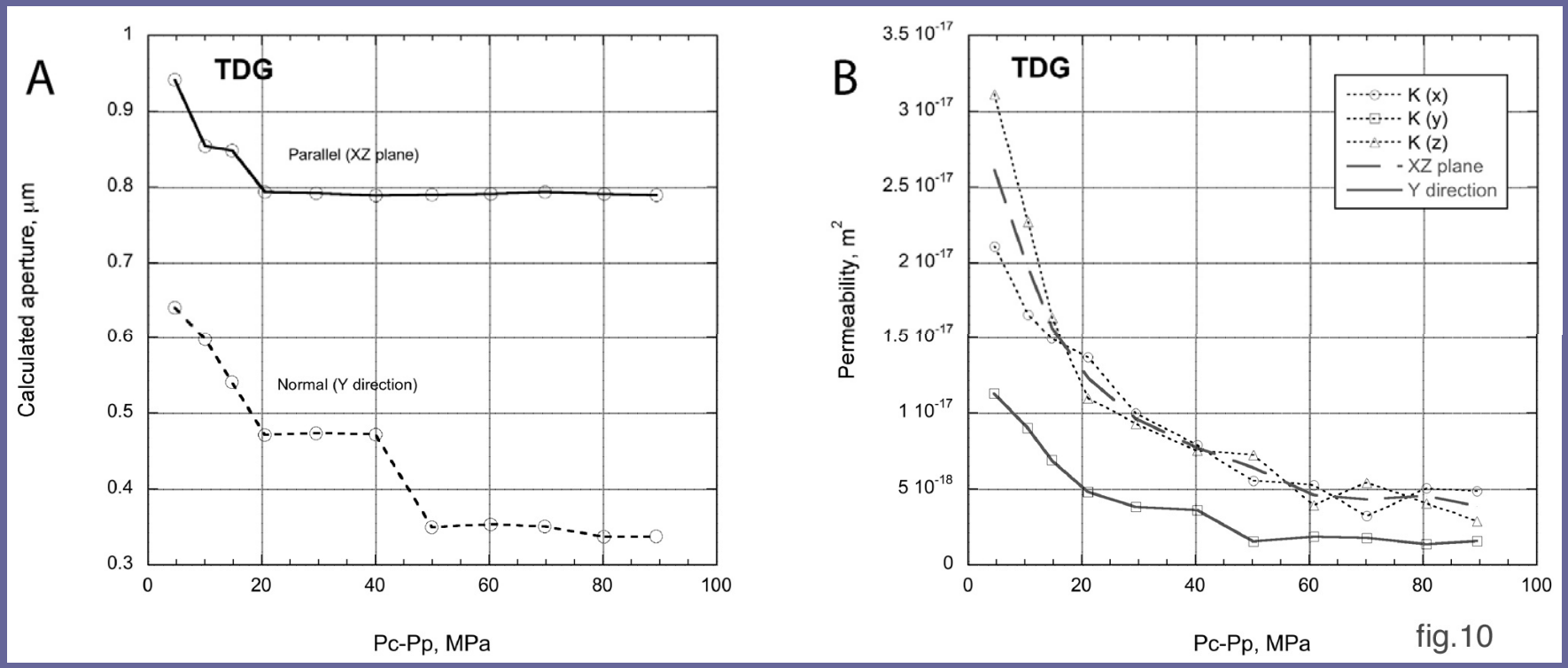

Calculated decrease in crack aperture with increase in effective pressure.

Comparison of measured (dotted lines) and modelled (dashed and solid lines) permeability.

Summary #2

- We have made contemporaneous measurements of changes in P and S wave velocities, porosity and permeability for rocks with different void space geometries as a function of effective pressure.
- We have used the Kachanov non-interacting crack model for transverse isotropy to estimate changes in crack density and aspect ratio from the velocity changes.
- We then use these estimates in each direction with the Gueguen & Dienes isotropic permeability model to forward model the sensitivity of permeability to variation in crack aperture as a function of increasing effective pressure.
- We conclude that, although there is an inherent background permeability in both rocks, the permeability variation can be explained by the variations in crack aperture.

#3 Permeability evolution during growth of compaction bands under triaxial stress

Sternlof, Rudnicki & Pollard, JGR, 2005.

- Compaction bands at different scales in sandstone formation, Utah
- Stand out after erosion due to high resistance to weathering
- Low porosity – grain crushing and high degree of cementation
- Low permeability – act as barriers to fluid flow barriers
- Sequences of bands compartmentalize fluid storage and flow

Experimental study using the large-volume triaxial deformation apparatus at UCL

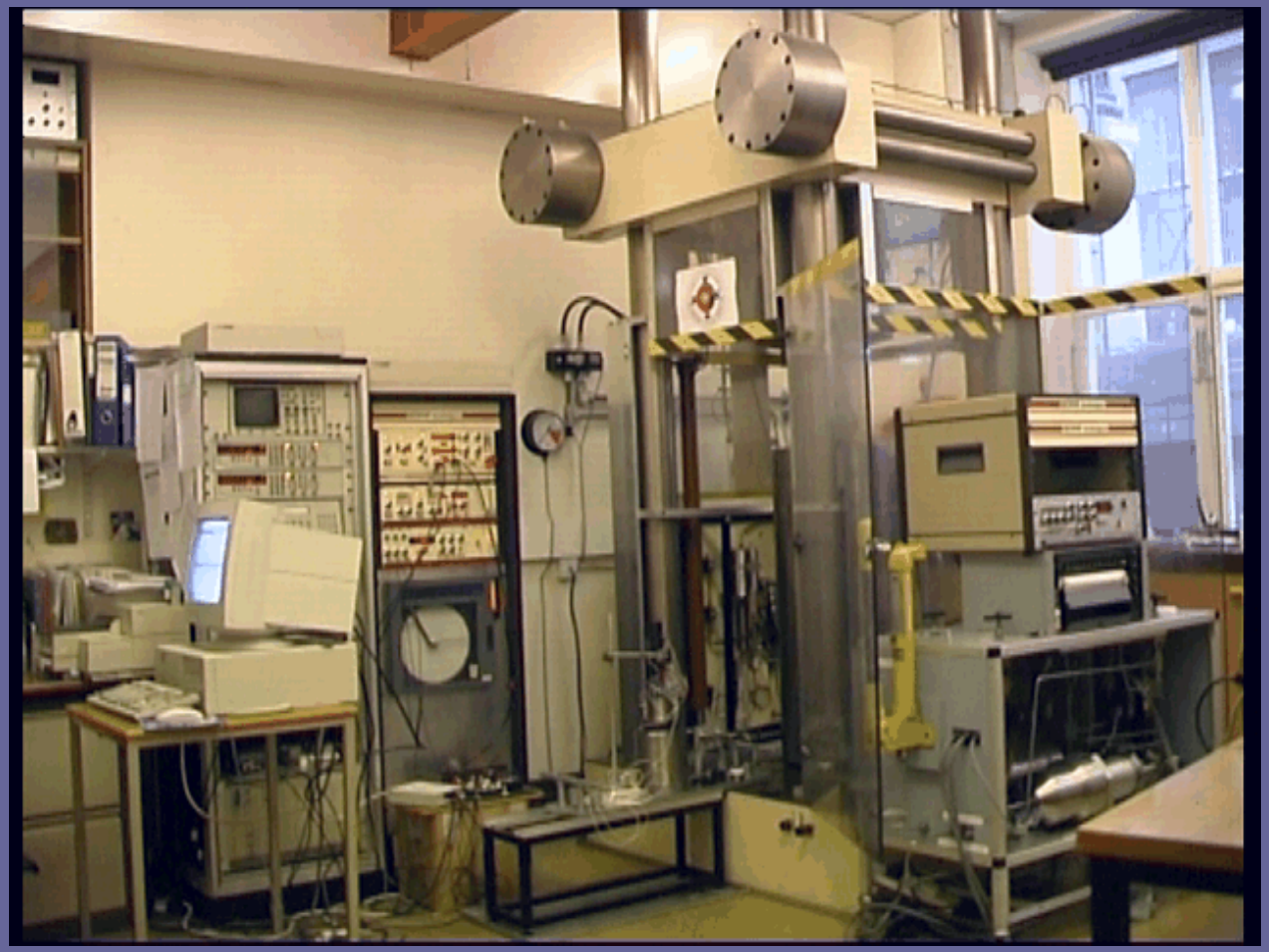

Conditions:

Drained triaxial tests

Constant pore pressure of 20 MPa

Constant strain rate of $10^{-5}s^{-1}$

Effective pressures from 10 to 250 MPa

3-D location of acoustic emission events

Sequential measurement of fluid permeability

Internal sample assembly:

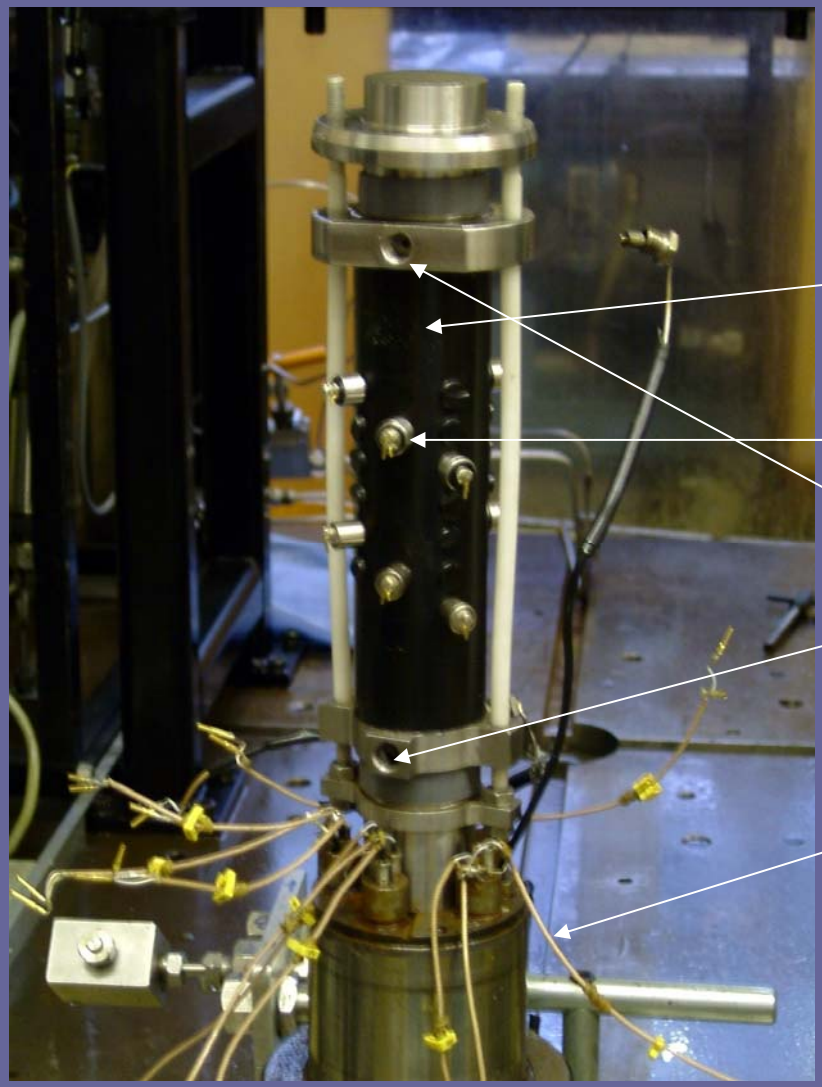

- Samples: 40mmϕ x 100mm
- Engineered nitrile jacket
- PZT AE transducers (12)
- Pore fluid inlet and outlet
- Co-axial cables to AE system

Test Material: Diemelstadt sandstone

Mineralogy	Texture
Quartz dominant (>60%)	Grain size 200 – 300 µm
Lithics common (~20%)	Subrounded - subangular
Feldspars rare (<10%)	Moderately sorted
Chlorite rare (~5%)	Porosity ~23%
Muscovite mica (trace)	
Heamatite staining (late)	

PPL XPL

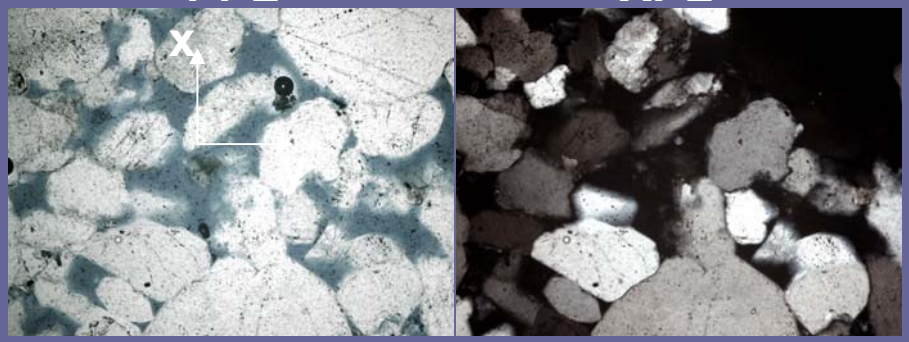

250 µm

- **Material is visibly anisotropic**
- **P-wave velocity anisotropy = 10%**
- **Transverse isotropy: oblate spheroid**

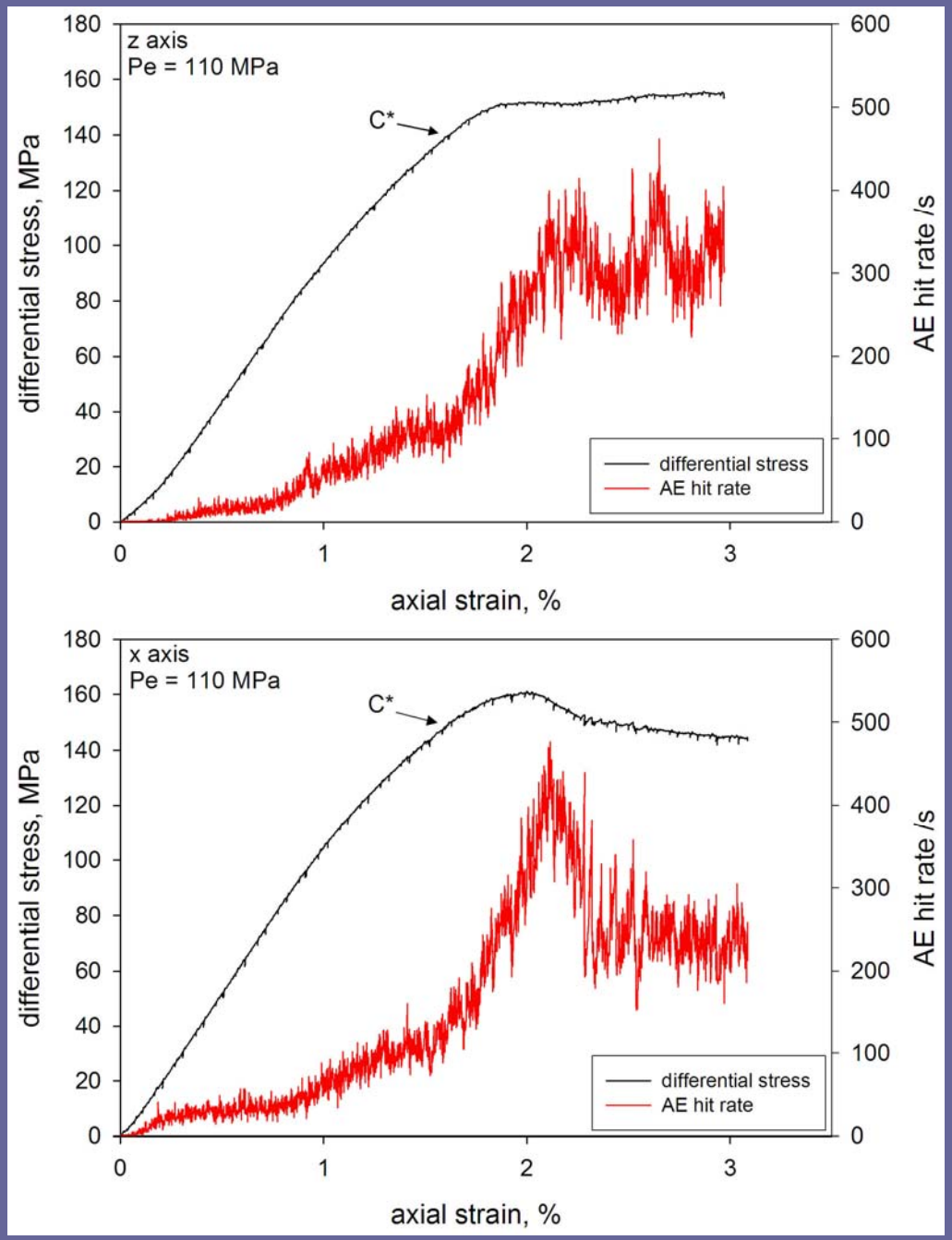

Z-axis samples:

Cored normal to bedding

Bands parallel to bedding

(C* marks the onset of shear-enhanced compaction)

X-axis samples:

Cored parallel to bedding

Bands normal to bedding

X-axis samples are consistently stronger than Z-axis samples

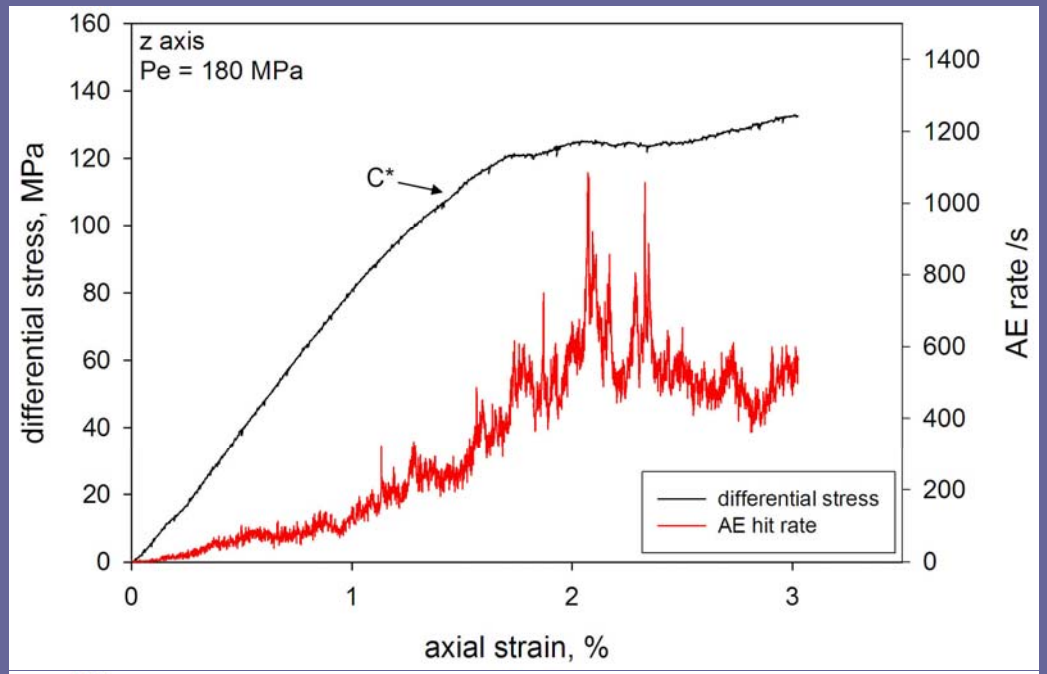

Z-axis data at an effective confining stress of 180 MPa

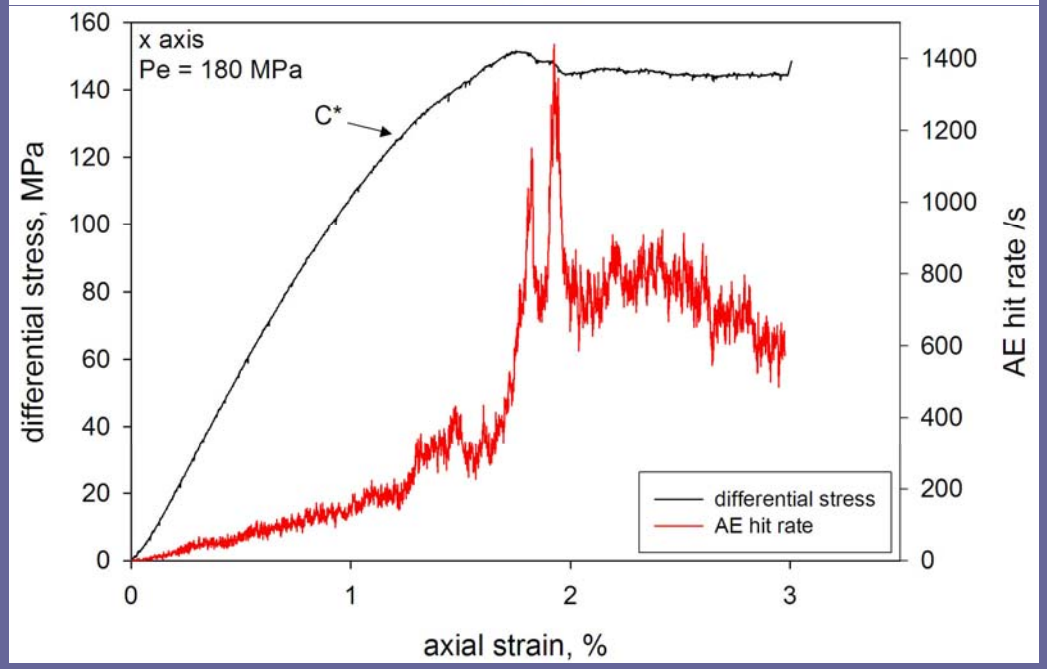

X-axis data for 180 MPa

Yield Surface in P-Q space:

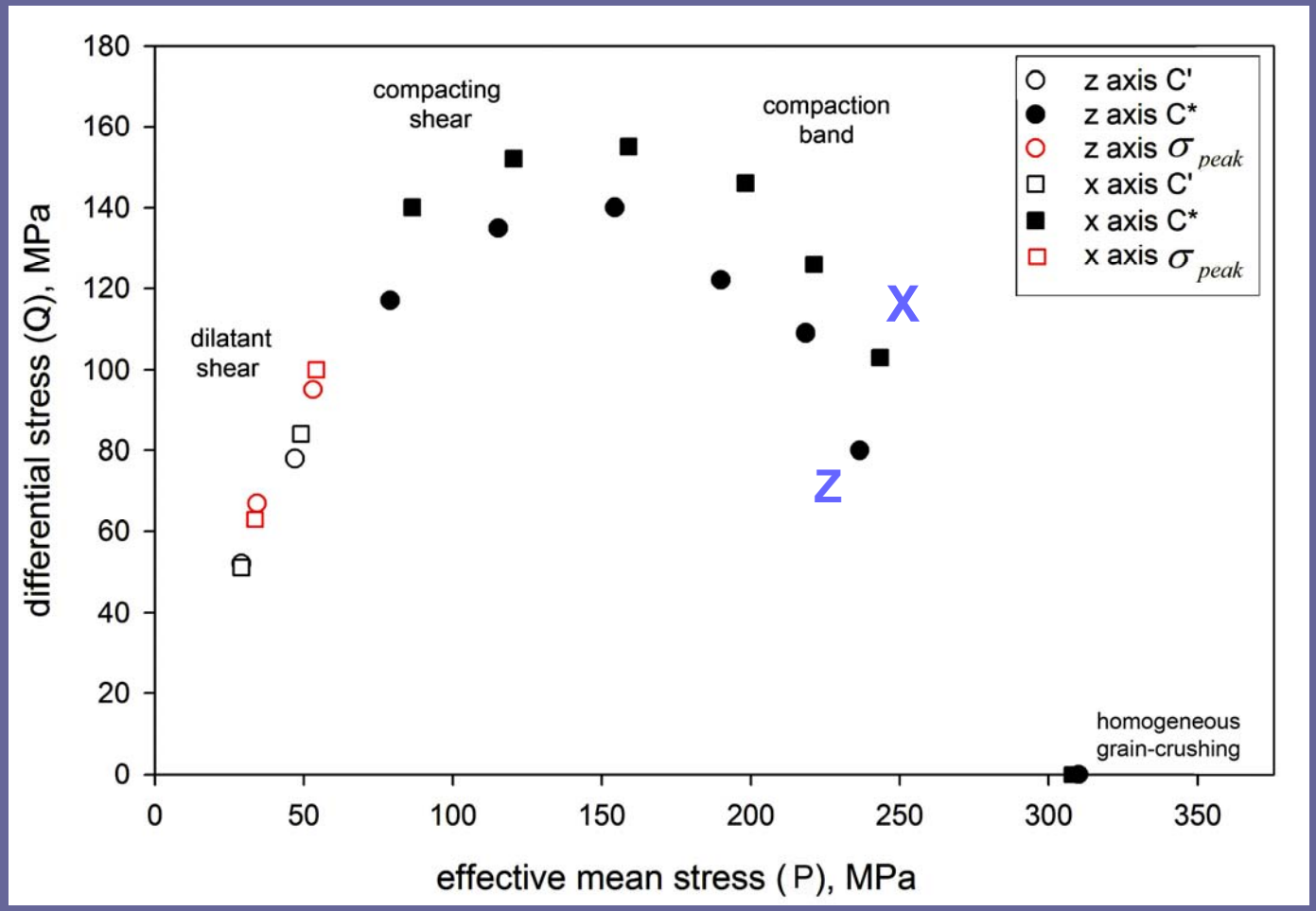

Permeability response to the growth of compaction bands:

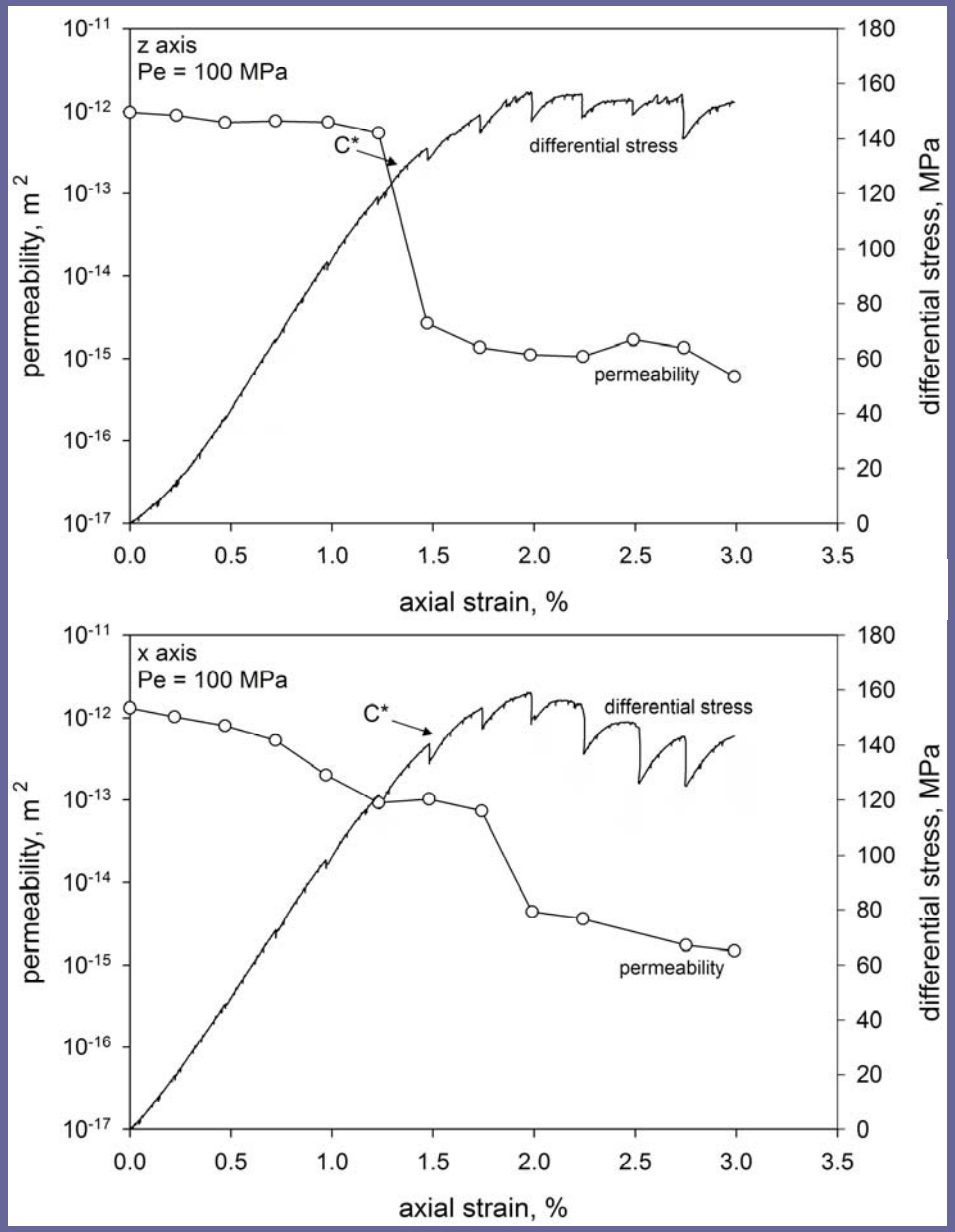

Z-axis cores:

Massive and rapid drop in K with growth of the first band.

Apparent reduction of 3 orders of magnitude (actually greater than 4 orders of magnitude).

More gradual reduction with growth of more bands

X-axis cores:

A similar overall reduction, but much more gradual.

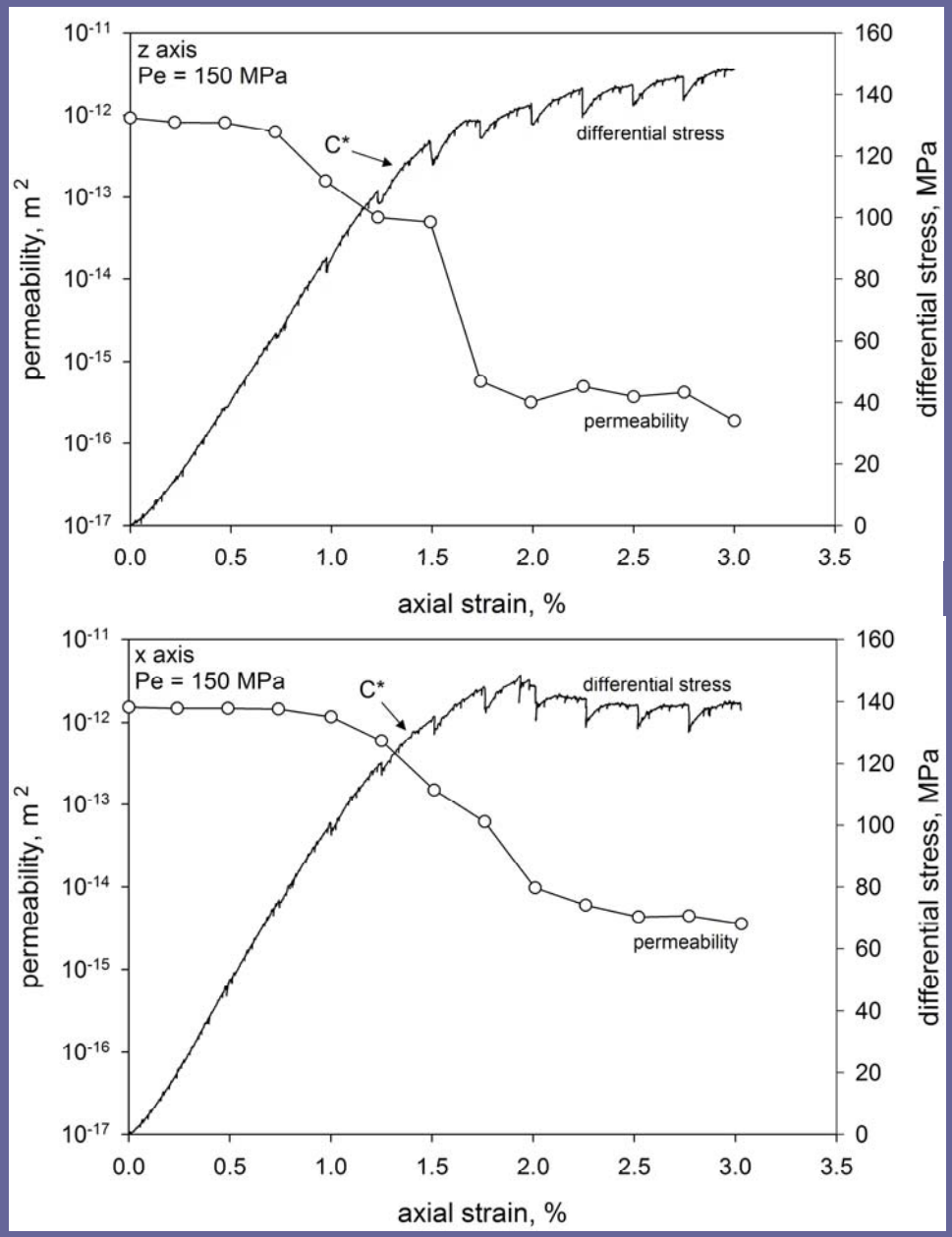

We observe similar behaviour in all experiments conducted in the compaction band regime.

This slide shows data for Z and X axis samples deformed at Pe = 150 MPa

How might we explain these observations?

Comparison of the geometry of Z and X axis bands:

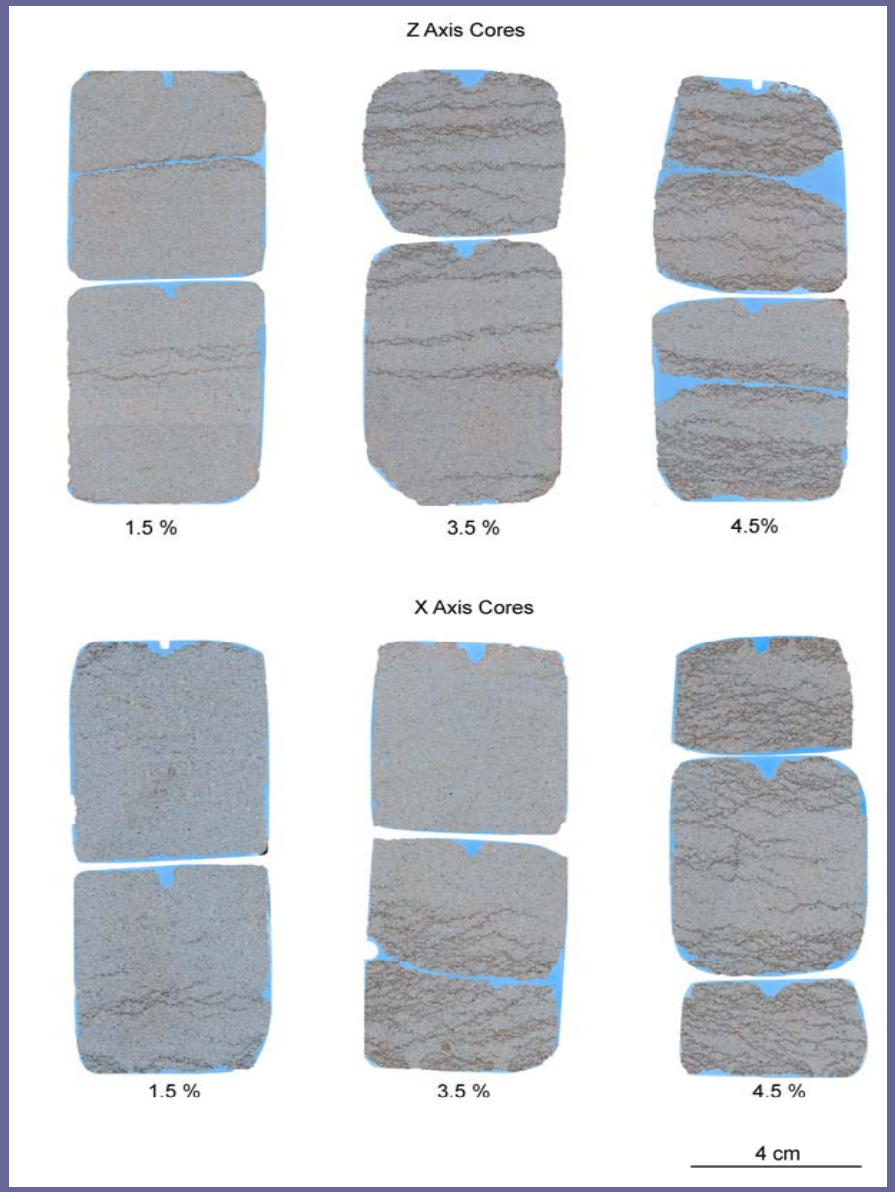

Bands in Z-axis cores grow along bedding. They are relatively straight, narrow and discrete.

Bands in X-axis cores grow across bedding. They are far more tortuous and diffuse.

This may explain both the different strength and the different permeability response.

Our observations are consistent with the predictions of the network model published by Katsman et al. (2005)

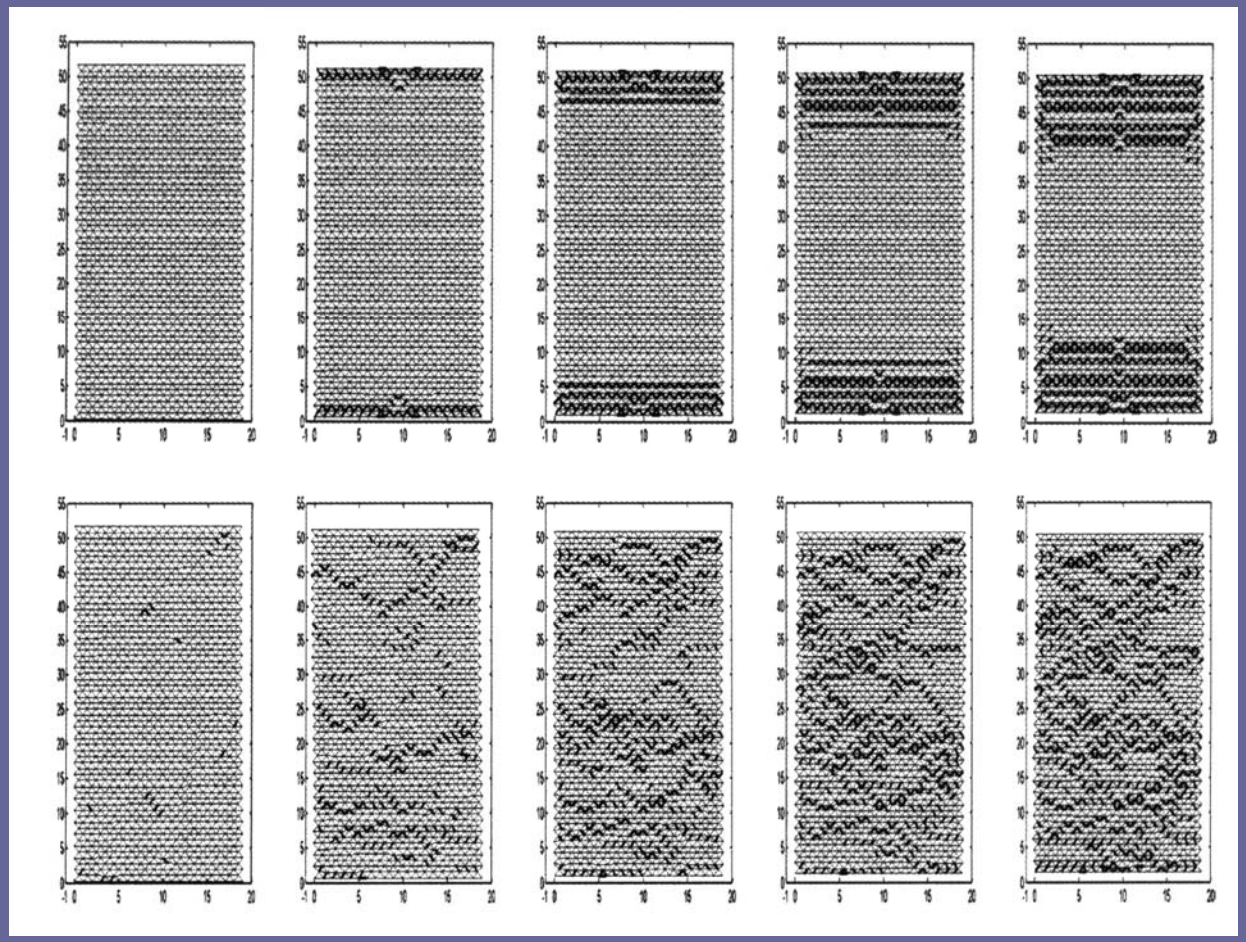

Homogeneous medium: Propagation of discrete compaction bands from the sample boundary.

Heterogeneous medium: Propagation of diffuse bands with damage nucleating in the interior of the sample.

Summary #3

- The style of compaction band propagation varies in anisotropic rocks.
- Bands propagating parallel to bedding are relatively straight, narrow and discrete.
- By contrast, bands propagating normal to bedding are far more tortuous and diffuse.
- Propagation of the first band results in a massive reduction in permeability of about 3 orders of magnitude.
- Since it is likely that permeability in the matrix does not change substantially, this implies a reduction of up to 5 orders of magnitude in the narrow (about 1mm) compaction band.
- Propagation of subsequent bands results in much smaller reduction; consistent with the layered effective medium model proposed by Vadjova, Baud & Wong, JGR, (2004).

END

Thank you for your attention

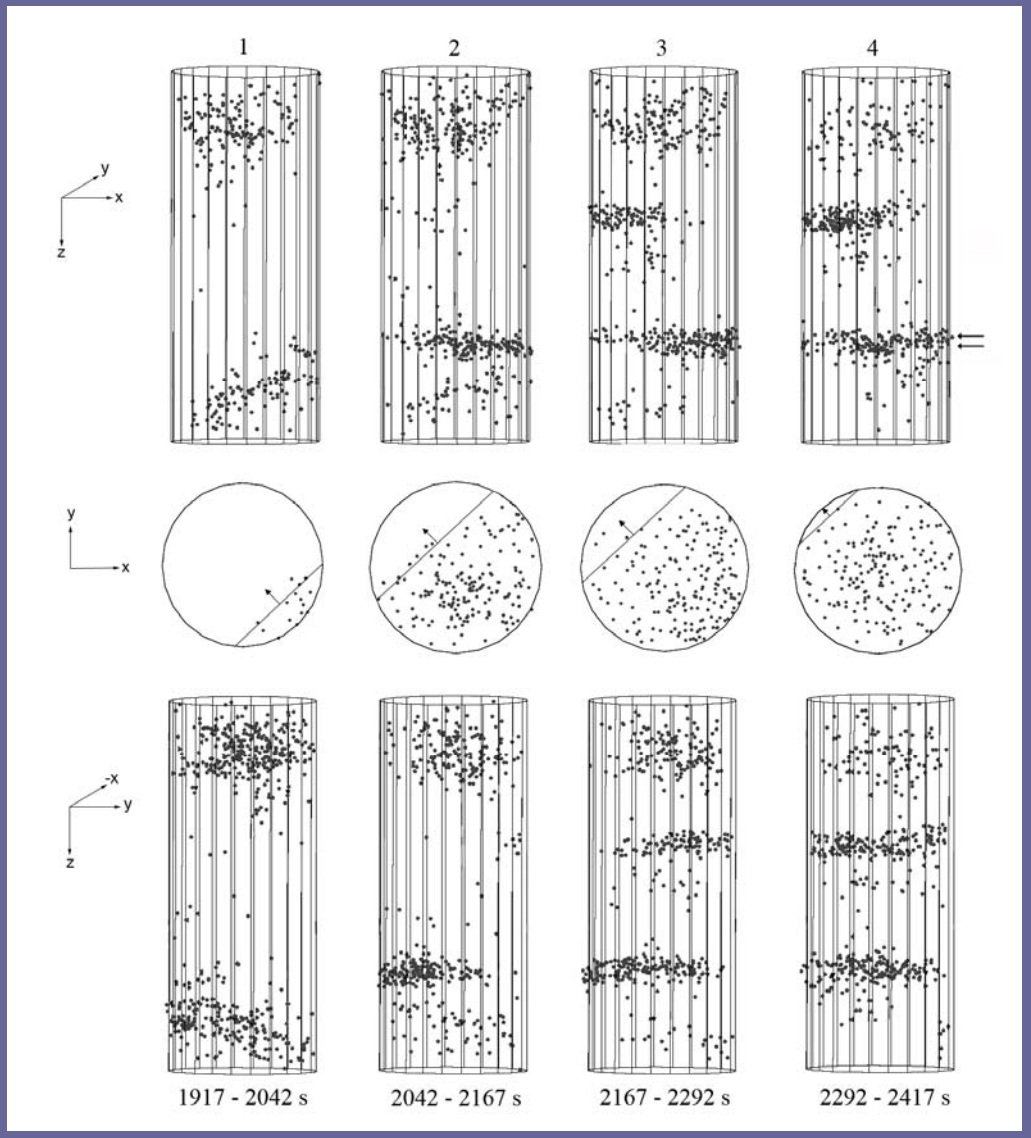
1
2
3
4
y
x
z
y
x
-x
y
z
1917 - 2042 s
2042 - 2167 s
2167 - 2292 s
2292 - 2417 s

3-D location of acoustic emission events

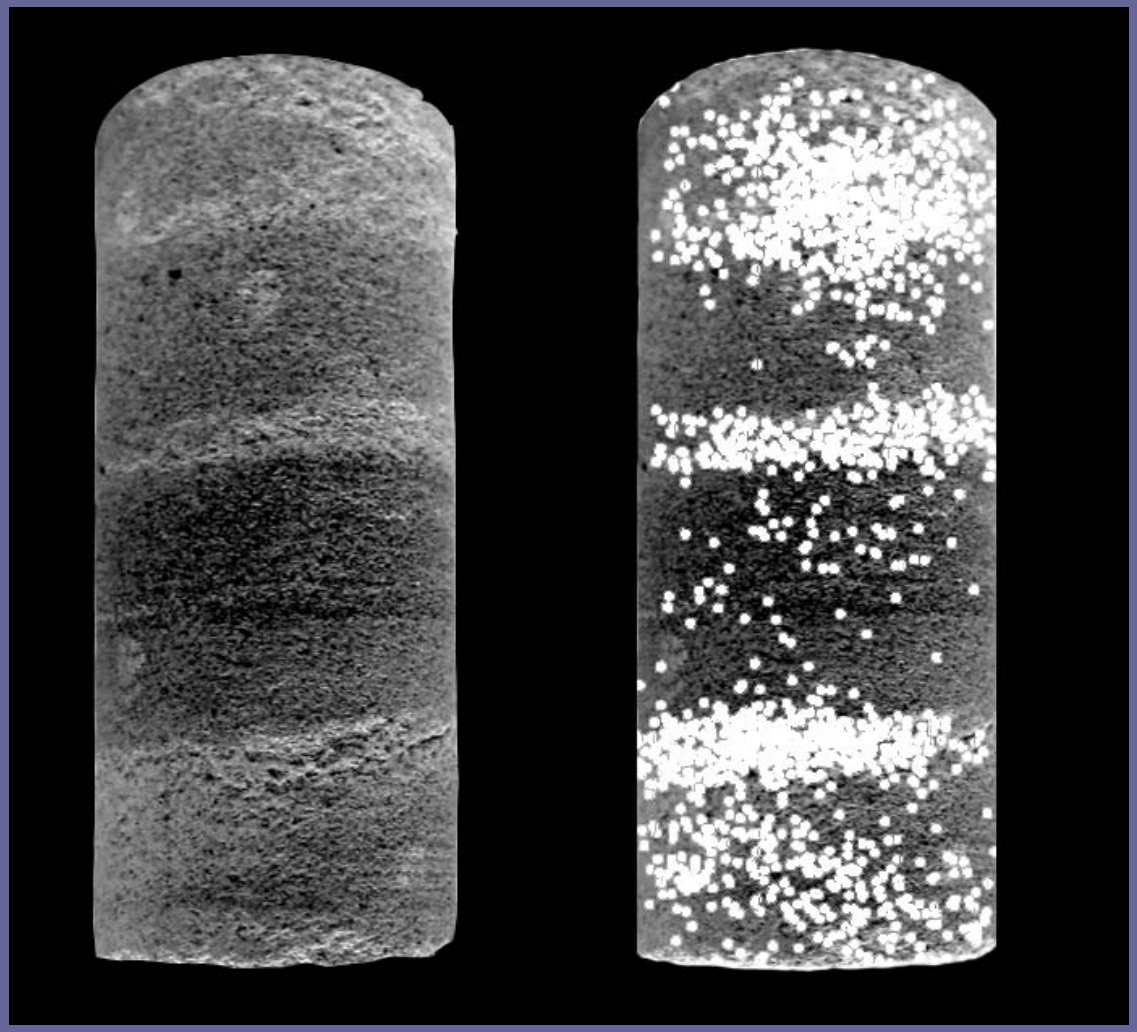

Z-axis sample deformed at Pe = 110 MPa

AE locations correspond to the locations of the propagating compaction bands

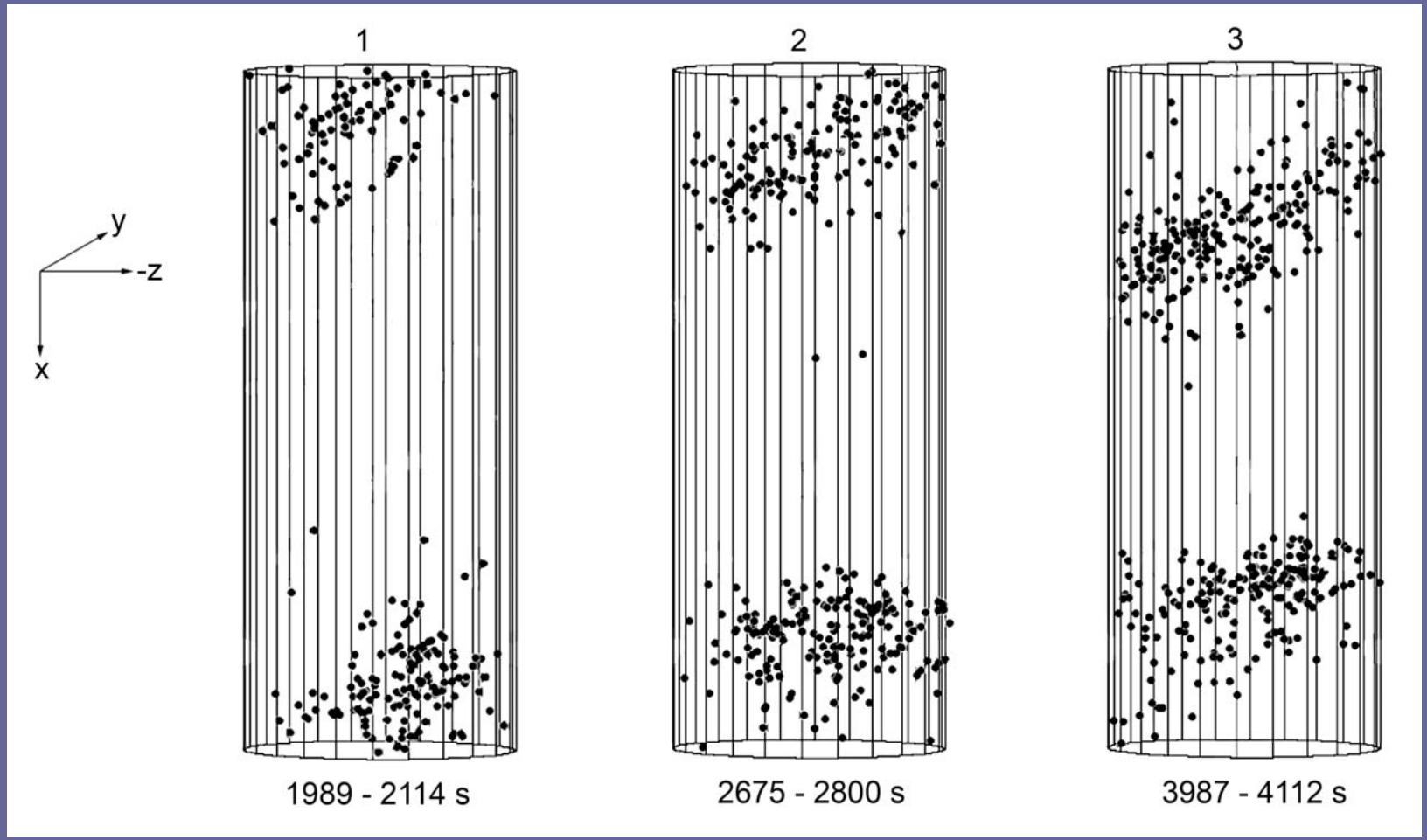
1
2
3
y
-z
x
1989 - 2114 s
2675 - 2800 s
3987 - 4112 s

Measurement Techniques

- Thermal stressing carried out by suspending samples in oven
- P and S wave velocities measured before and after thermal stressing using time-of flight method
- Permeameter uses Confining Pressures = 20 - 100MPa, Pore Pressure = 10MPa and ΔP = 10MPa. Room Temperature (varies between 19°C and 21°C) and pore fluid is deionised water
- Balanced steady-state flow technique
- Measurements take between 1 hour and 2 weeks
- Permeability calculated from flow rates and Darcy equation

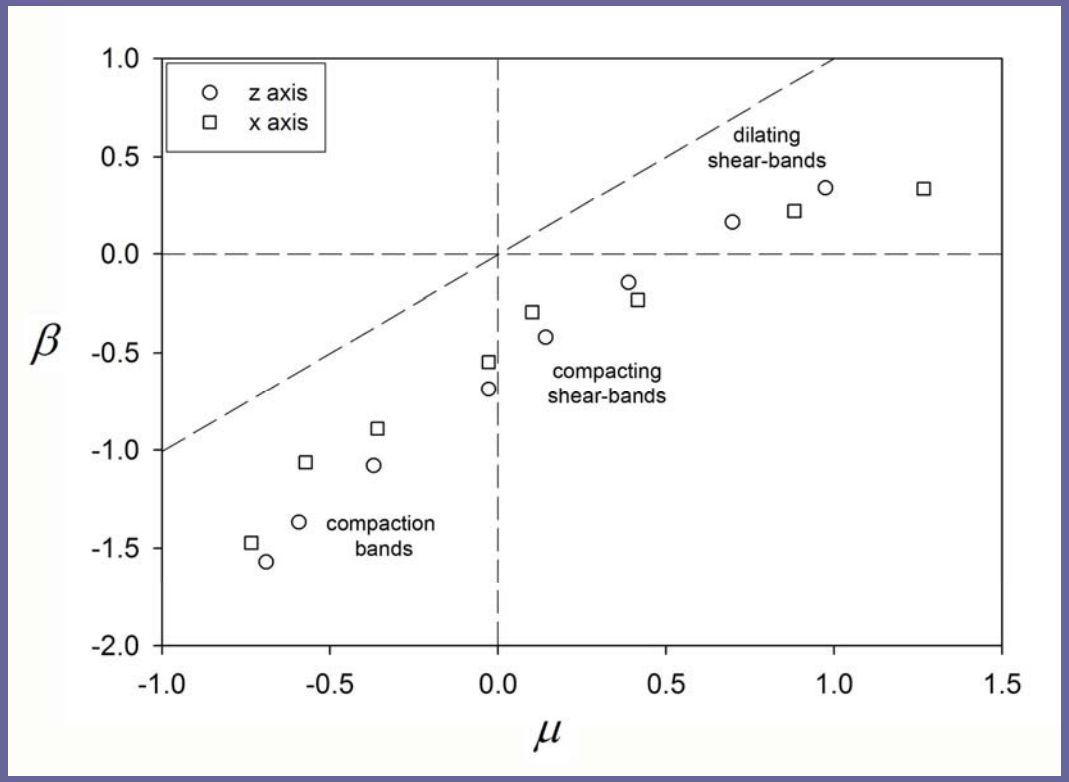
z axis
x axis
dilating
shear-bands
compacting
shear-bands
compaction
bands
1.0
0.5
0.0
-0.5
-1.0
-1.5
-2.0
-1.0
-0.5
0.0
0.5
1.0
1.5
β
μ